AIP | Applied Physics Letters

Excitonic bandgap dependence on stacking configuration in four layer graphene

Y. P. Liu, S. Goolaup, W. S. Lew, I. Purnama, M. Chandra Sekhar, T. J. Zhou, and S. K. Wong

Citation: Applied Physics Letters **103**, 163108 (2013); doi: 10.1063/1.4825263
View online: http://dx.doi.org/10.1063/1.4825263
View Table of Contents: http://scitation.aip.org/content/aip/journal/apl/103/16?ver=pdfcov
Published by the AIP Publishing

Excitonic bandgap dependence on stacking configuration in four layer graphene

Y. P. Liu,[1] S. Goolaup,[1] W. S. Lew,[1,a)] I. Purnama,[1] M. Chandra Sekhar,[1] T. J. Zhou,[2] and S. K. Wong[2]
[1]*School of Physical and Mathematical Sciences, Nanyang Technological University, 21 Nanyang Link, Singapore 637371*
[2]*Data Storage Institute, A*STAR (Agency for Science Technology and Research), 5 Engineering Drive 1, Singapore 117608*

(Received 22 July 2013; accepted 23 September 2013; published online 16 October 2013)

Different crystallographic stacking configurations in graphene provide an additional degree of freedom in the electronic structure. We have conducted systematic investigations of the transport properties of ABAB- and ABCA-stacked four-layer graphene. Our results reveal that ABAB and ABCA graphene exhibit markedly different properties as functions of both temperature and magnetic field. The temperature-dependant resistance measurement reveals that the excitonic gap of ABCA stacked graphene increases as a function of temperature, while for ABAB, a shrinking excitonic gap configuration is observed. © *2013 AIP Publishing LLC*. [http://dx.doi.org/10.1063/1.4825263]

Research in graphene is motivated by both the interesting physics and an optimistic prospective of device engineering.[1,2] Graphene exhibits intriguing electronic properties; its low-energy excitations are massless, chiral, Dirac fermions.[3–7] Recently, the focus on graphene study is gradually being extended to structures with higher number of layers or few-layer graphene (FLG). In FLG, there exist different crystallographic stacking configurations,[8] e.g., AA and AB for bilayer, ABC and ABA for trilayer, ABCA and ABAB for four-layer, and ABCAB and ABABA for five-layer graphene, providing an additional degree of freedom.[9–12] The different stacking configurations are expected to modify the bandgap structure[13–15] and complicate the electronic interactions in FLG.[16–18] Electronic transport behaviour, which not only differs from that observed in mono- and bilayer graphene, is anticipated to be observed in FLG with different stacking configuration, albeit with similar number of graphene layer.[8–10] In trilayer graphene, for instance, Bernal (ABA)-stacked trilayer is predicted to have a tuneable bandgap with semimetallic property, while rhombohedral (ABC)-stacked trilayer exhibits a tuneable gap leading to insulating property.[19–21] In four layer graphene, there is 16-fold Landau Level (LL) degeneracy at zero energy.[22,23] Moreover, the electronic structure and the LL spectrum differ significantly depending on the stacking order in four-layer graphene.[8] To date, it still remains an open question on how the nature of ABAB and ABCA stacking configurations can affect the electronic transport properties of four-layer graphene. In this letter, we present investigations on the magneto-transport behaviour in pure ABAB- and ABCA-stacked four-layer graphene structures. Our temperature-dependent magnetoresistance (MR) measurements reveal that the excitonic gap in ABCA-stacked graphene undergoes expansion, whereas that in ABAB-stacked graphene exhibits retracting property.

The four-layer graphene samples were prepared using mechanical exfoliation techniques.[2] Graphene flakes were extracted from bulk highly oriented pyrolytic graphite (grade ZYA, SPI Supplies) by sticky tapes and then transferred onto the surface of a lightly doped silicon substrate that was covered with a 300-nm-thick SiO_2 layer. A WITEC CRM200 microscope, operating at 532 nm excitation wavelength in the back-scattering configuration,[24] was used to measure the Raman spectra of the graphene samples at room temperature.[25–28] Shown in Fig. 1(a) is the characteristic Raman spectrum of the four-layer graphene. The two most intense features which are the G peak and the 2D band are sensitive to the number layers of graphene. The number of graphene layer can be confirmed by comparing the position of the G peaks and the shape of the 2D bands while the full width half maximum of the 2D band can provide another method of graphene layer comparison. Inset in Fig. 1(a) shows a close-up view of the D peak region. Although the D peak intensity observed in the Raman spectra is relatively small, it indicates the presence of intervalley scatterers, which is the key contributor to the weak localization effect (WL) in graphene.[29] Atomic force microscope (AFM) measurement was performed to check the thickness of the four-layer graphene. Fig. 1(b) shows the AFM image with cross-sectional height profiles. The measured height is 1.715 nm, which is slightly larger than the theoretical value of (0.334 nm × 4 =) 1.336 nm. The 0.379 nm thickness discrepancy is ascribed to a "dead" space between the graphene and the SiO_2 substrates.[2,3] To identify the layer stacking configuration in the four-layer graphene, Raman 2D-mode mapping technique was used.[30] In Fig. 1(c), the scanned images of Raman 2D-mode mapping are shown. The red and yellow spectra shown in the images correspond to ABAB and ABCA four-layer graphene domains, respectively. In the process of preparing different stacking configurations four-layer graphene samples, we consistently obtained 80% ABAB stacking, and 20% ABCA stacking.

A standard four-terminal configuration was used for graphene electrical transport characterization. Four Cr (10 nm)/Au (80 nm) electrical contact electrodes were patterned using photolithography technique, and the metallic films were deposited by thermal evaporation at a base pressure

a)Author to whom correspondence should be addressed. Electronic mail: wensiang@ntu.edu.sg. Tel.:+65 63162963. Fax: +65 67957981.

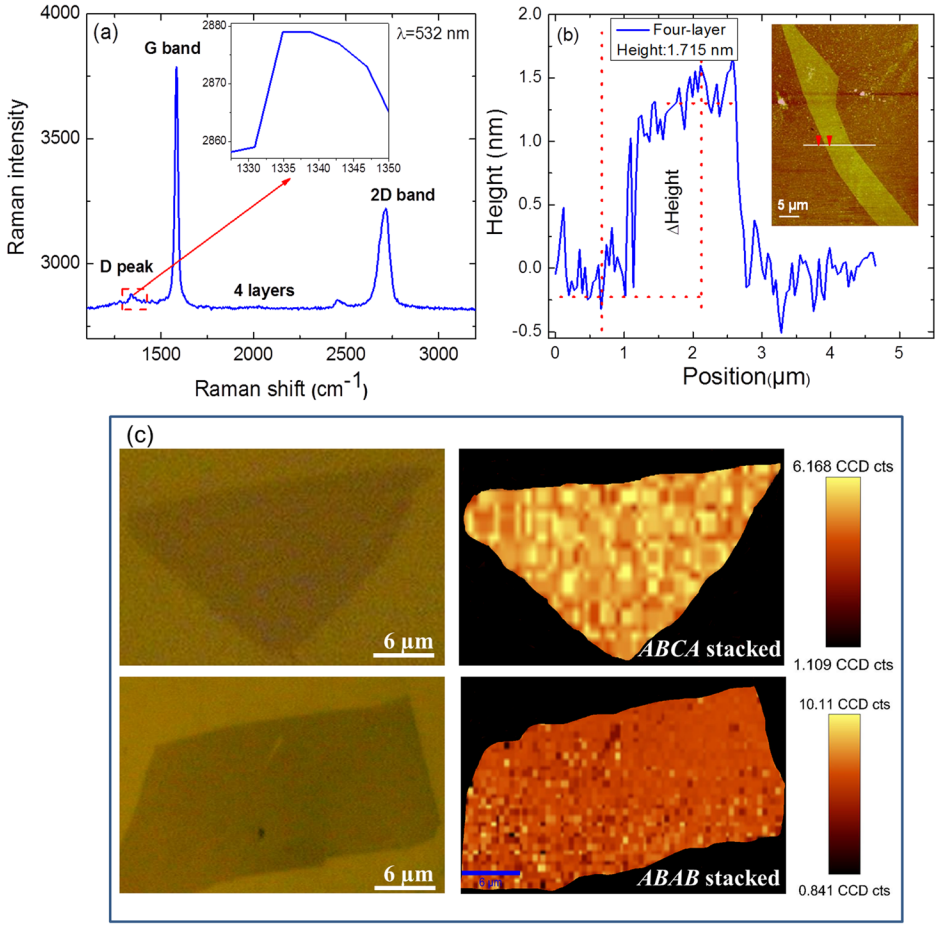

FIG. 1. (a) Raman spectra of four-layer graphene at 532 nm. Inset is a close-up view of the D peak region. The G peak position and the 2D band features are useful to confirm the number of graphene layer. (b) AFM cross-sectional profile of the four-layer graphene. The measured height of the investigated graphene sample is 1.715 nm. (c) Raman 2D-mode mapping spectra of ABCA and ABAB stacked four-layer graphene. The yellow and red regions in the images correspond to ABCA and ABAB four-layer graphene domains, respectively.

of 10^{-7} millibars, with a subsequent lift off in warm acetone. The inset in Fig. 2(a) shows an optical image of the four layer graphene with corresponding Cr/Au contact electrodes. The graphene samples were annealed at 300 °C in low vacuum condition for 1 h to eliminate surface contamination. *In situ* graphene device cleaning by electric field was also performed to improve the measurement quality. The transport measurements were carried out by a physical property measurement system (PPMS, Quantum Design). The measurements were performed in the temperature range of 2–340 K and a magnetic field of 0–12 T was applied.

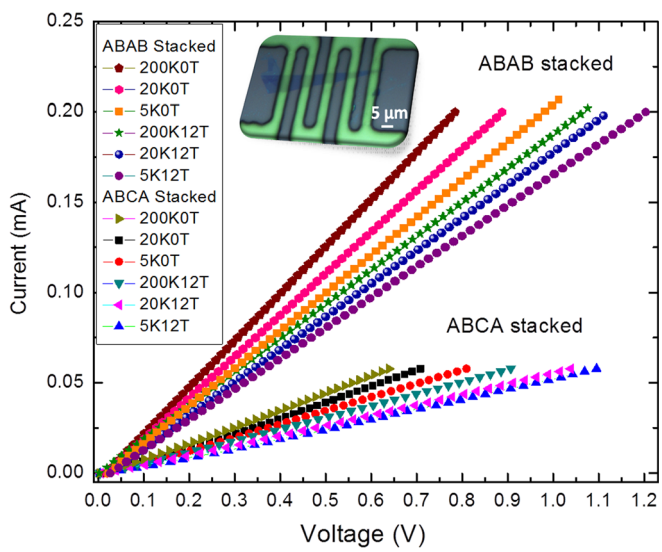

FIG. 2. (a) Temperature-dependent current-voltage characteristics of ABAB- and ABCA- stacked order four-layer graphene. Inset is an optical micrograph of the four-layer graphene with four Cr/Au contact electrodes. The measurements show that the four-layer graphene has intrinsic semiconductor property and the application of a perpendicular magnetic field has induced higher electrical resistance in the graphene layer.

The current-voltage (I-V) measurements of the ABAB and ABCA four layer graphene with an out of plane magnetic field is presented in Figure 2(a). Both the ABAB and ABCA four-layer graphene exhibit a linear I-V relationship, indicating the ohmic nature of the graphene samples. However, there is a marked difference in the resistance, the reciprocal of the gradient of the measured I-V plot, of the two stacking graphene samples. The ABAB-stacked graphene exhibits a larger resistance value as compared to the ABCA-stacked graphene for all the field strengths and temperatures investigated. Both crystallographic stacking configurations exhibit a decrease in resistance as a function of temperature, a characteristic of intrinsic semiconductor.

Under the application of an external magnetic field, the resistance of the four-layer graphene increases. The dependence of the graphene resistance on the magnetic field strength suggests that the graphene resistance is a qualitative indication of its excitonic gap, the opening of gap as a result of LL splitting. In four layer graphene, there exist 16 zero-energy levels.[33] Sensitivity of the four-layer graphene to the magnetic field is more pronounced, giving rise to larger spacing of the energy levels. Independent of the number layers, the energy levels $N \neq 0$ are all four-fold, where two fold arises from the electron spin and two fold from the valley degeneracy. High field (0–12 T) MR measurements of both ABCA- and ABAB-

stacked graphene were carried out. Figs. 3(a) and 3(b) show the measured MR ratio at different temperatures, using the resistance R (B = 0 T, T = 5 K) as the denominator. The monotonic increase in resistance with increasing applied magnetic field strength is a clear signature of the formation of graphene bands structure due splitting LL. Fig. 3(e) depicts an illustration of the LL splitting under the influence of a magnetic field. Under an applied magnetic field, an excitonic gap is formed due to the attractive interaction between electron-hole pairs.[22–31] The presence of the excitonic gap indicates the breaking of sub-lattice symmetry.[31–33] The excitonic gap shows thermally driven property and it also depends on the strength of applied magnetic field.

To probe the quantum electronic behaviour at low temperature, specifically for the weak localisation effect, low field magnetoresistance measurements were carried out and the results are shown in Figs. 3(b) and 3(d). A negative magneto-resistive behaviour is observed, which is a characteristic of the WL. The WL effect originates from the intervalley scattering induced by resonant scatterers.[29,34,35] The magnitude of the negative MR for both stacking configuration graphene decreases as the temperature rises, due to the reduction of the phase coherence time. At low temperatures, the elastic scattering is dominant, enabling electron to retain their phase coherence over a long distance. As temperature increases, inelastic scattering dominates, resulting in the phase coherence distance of electron wave becoming smaller than the scattering length.[36–38] The study of the WL effect in mono- and bilayer graphene has been relatively established but in the investigated four-layer graphene the observed WL effect displays a stronger enhancement. At first glance, there is no significant difference in the WL effect observed for the two stacking four-layer graphene. However, as the temperature rises, the measurement revealed that the field at which the minima of the negative MR occurs is different for the two stacking configurations. Specifically, at 200 K, there is a ~0.3 T minima field difference between the ABCA-stacked and the ABAB-stacked graphene. The origin of the field minima shift is attributed to the rhombohedral (ABCA) like systems having flatter bands than Bernal (ABAB) stacking. As a result, the density of states is higher, and they are more prone to instabilities.

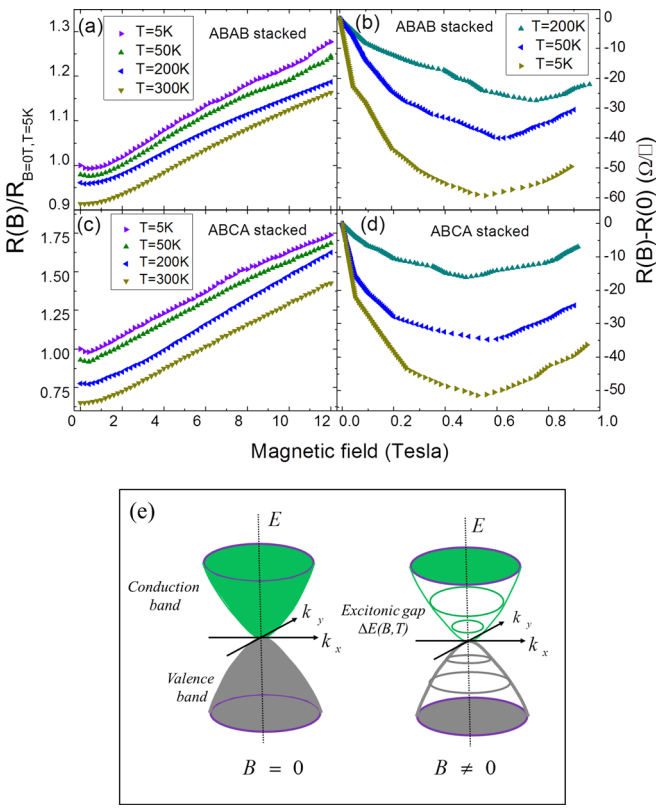

FIG. 3. Resistance measurements in four-terminal configuration as a function of magnetic field at different temperatures. Plots (a) and (c) are the high field magnetoresistance measurement of ABAB- and ABCA-stacked four-layer graphene. Plots (b) and (d) are low-field magnetoresistance measurement of ABAC- and ABAB-stacked graphene. The observed negative magnetoresistive behaviour is a characteristic of the weak localization effect. (e) Illustration of four-layer graphene Landau level splitting under the application of a magnetic field. The zero-energy state with respect to up-spin electrons and down-spin holes make an excitation gap due to the attractive Coulomb force between a hole and an electron.

Figs. 4(a) and 4(c) show the measured resistance of the four-layer graphene as a function of temperature, under the influence of different magnetic field strengths. The resistance is normalised to the value of $R_{B=0\ T,\ T=5\ K}$. As the temperature increases from 5 to 340 K, the measured resistance of the four-layer graphene drops gradually, exhibiting semiconductor type behaviour. The decreasing resistance with increasing temperature suggests that impurity Coulomb scattering is the dominant scattering mechanism in the four-layer graphene.[39] The trend of the plot can be explained using a combination of the individual resistance component arising from the two scattering mechanisms ($R_{Four\text{-}layer} = R_{Coulomb} + R_{Short\text{-}range}$), where $R_{Coulomb}$ and $R_{Short\text{-}range}$ are the resistance components from Coulomb and short range scattering mechanisms, respectively. The short range resistance ($R_{Short\text{-}range}$) is independent of temperature,[38] while the Coulomb resistance ($R_{Coulomb}$) is shown to decrease with respect to increasing temperature.

We have discussed earlier that the induction of higher resistance when a magnetic field is applied can infer the excitonic gap opening property. To further study this feature, the

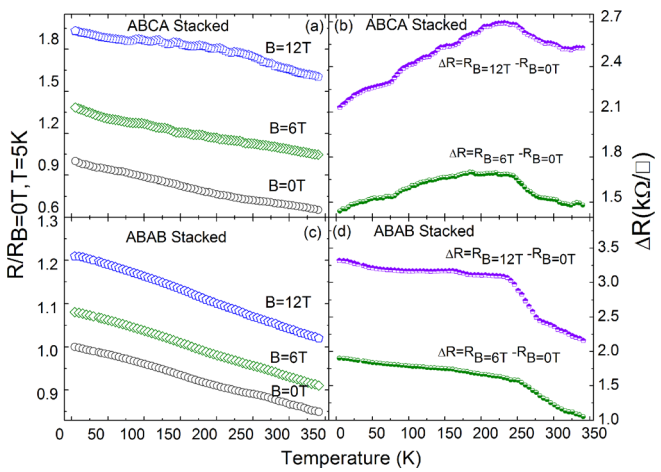

FIG. 4. Normalized magnetoresistance of (a) ABCA- and (b) ABAB-stacked graphene as a function of temperature. The results show that when the temperature increases from 5 to 340 K, the resistance of the two stacking configurations graphene drops following the behaviour of a semiconductor. Relative resistance change values ($\Delta R = R_B - R_{B=0T}$) are plotted as a function of temperature for (c) ABCA- and (d) ABAB-stacked graphene. The results clearly differentiate the thermally activated electronic behaviour of the two crystallographic stacking graphene.

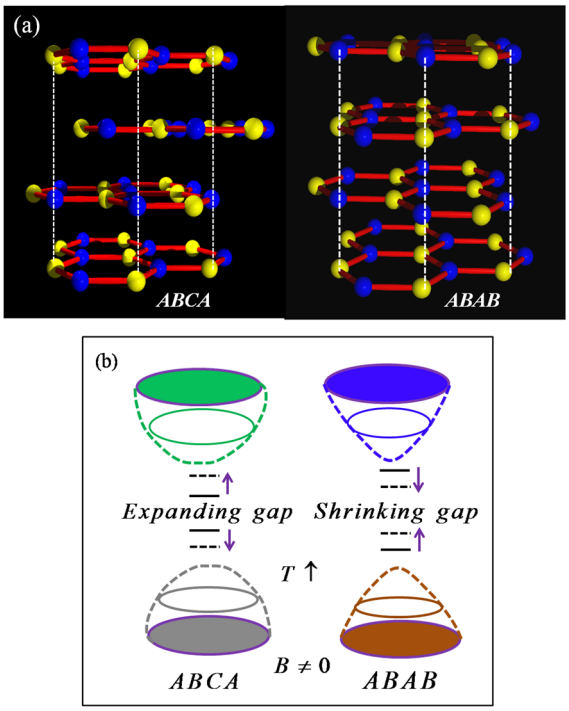

FIG. 5. (a) Illustration of the crystallographic structure of ABCA- and ABAB-stacked four-layer graphene. (b) Schematic showing the expanding and retracting excitonic gap behaviour in each stacking configuration of the four-layer graphene when under the influence of perpendicular magnetic fields and rising temperatures.

relative resistance change values $\Delta R = R_{B=6T,12T} - R_{B=0T}$ of both ABCA and ABAB stacking four-layer graphene were extracted from the *R-T* measurements and plotted as a function of increasing temperature, as shown in Figs. 4(b) and 4(d). For ABCA-stacked graphene, the ΔR value increases as temperature rises, up to ~230 K where the ΔR drops thereafter. The ΔR value can be qualitatively interpreted as the "expansion" of the excitonic gap. However, for ABAB-stacked graphene, a decreasing ΔR is observed. The decreasing ΔR value indicates an excitonic gap that is retracting as temperature rises, until ~230 K (or 250 K for 6 T data) where the ΔR drops thereafter. Illustration of the atomic arrangement of ABCA- and ABAB-stacked four-layer graphene is shown in Fig. 5(a). Shown in Fig. 5(b) is the schematic showing the effects of applying magnetic field and changing the temperature of the four layer graphene.

In conclusion, systematic investigations of the transport properties under the influence of temperature and magnetic fields have been conducted in ABAB- and ABCA-stacked four-layer graphene. Our results reveal that ABAB and ABCA graphene configurations exhibit distinctively different properties as functions of temperature and magnetic field. The obtained results provide a qualitative proof of the theoretically predicted field-induced excitonic gap. The temperature-dependant resistance measurement reveals that the excitonic gap of ABCA stacked graphene increases as a function of temperature. For ABAB, a shrinking excitonic gap configuration is observed. Potentially, the observed phenomena provide an important transport information to the design of four-layer graphene magnetic sensor that can be manipulated by a magnetic field.

This work was supported in part by the NRF-CRP program (Multifunctional Spintronic Materials and Devices). The authors thank Professor F. Guinea for helpful discussion, and Zhang Mingsheng (A*STAR) and Sun Li for their assistance in experimental measurements.

[1]A. K. Geim and K. S. Novoselov, Nature Mater. **6**, 183 (2007).
[2]K. S. Novoselov, A. K. Geim, S. V. Morozov, D. Jiang, Y. Zhang, S. V. Dubonos, I. V. Grigorieva, and A. A. Firsov, Science **306**, 666 (2004).
[3]K. S. Novoselov, A. K. Geim, S. V. Morozov, D. Jiang, M. I. Katsnelson, I. Grigorieva, S. V. Dubonos, and A. A. Firsov, Nature **438**, 197 (2005).
[4]D. S. L. Abergel, V. Apalkov, J. Berashevich, K. Ziegler, and T. Chakraborty, Adv. Phys. **59**, 261 (2010).
[5]N. M. R. Peres, Vacuum **83**, 1248 (2009).
[6]P. R. Wallace, Phys. Rev. **71**, 622 (1947).
[7]A. K. Geim, Science **324**, 1530 (2009).
[8]M. Aoki and H. Amawashi, Solid State Commun. **142**, 123 (2007).
[9]A. I. Cocemasov, D. L. Nika, and A. A. Balandin, Phys. Rev. B **88**, 035428 (2013).
[10]K. F. Mak, J. Shan, and T. F. Heinz, Phys. Rev. Lett. **104**, 176404 (2010).
[11]S. Latil and L. Henrard, Phys. Rev. Lett. **97**, 036803 (2006).
[12]W. Norimatsu and M. Kusunoki, Phys. Rev. B **81**, 161410 (2010).
[13]F. Guinea, A. H. C. Neto, and N. M. R. Peres, Phys. Rev. B **73**, 245426 (2006).
[14]A. A. Avetisyan, B. Partoens, and F. M. Peeters, Phys. Rev. B **80**, 195401 (2009).
[15]A. A. Avetisyan, B. Partoens, and F. M. Peeters, Phys. Rev. B **81**, 115432 (2010).
[16]M. Koshino, Phys. Rev. B **81**, 125304 (2010).
[17]M. Otani, M. Koshino, Y. Takagi, and S. Okada, Phys. Rev. B **81**, 161403 (2010).
[18]E. McCann and M. Koshino, Phys. Rev. B **81**, 241409 (2010).
[19]C. H. Lui, Z. Q. Li, K. F. Mak, E. Cappelluti, and T. F. Heinz, Nat. Phys. **7**, 944 (2011).
[20]W. Bao, L. Jing, J. Velasco, Jr., Y. Lee, G. Liu, D. Tran, B. Standley, M. Aykol, S. B. Cronin, D. Smirnov, M. Koshino, E. McCann, M. Bockrath, and C. N. Lau, Nat. Phys. **7**, 948 (2011).
[21]Y. P. Liu, S. Goolaup, C. S. Murapaka, W. S. Lew, and S. K. Wong, ACS Nano **4**, 7087 (2010).
[22]M. Ezawa, J. Phys. Soc. Jpn. **76**, 094701 (2007).
[23]A. J. M. Giesbers, L. A. Poromarenko, K. S. Novoselov, A. K. Geim, M. I. Katnelson, J. C. Maan, and U. Zeitler, Phys. Rev. B **80**, 201403 (2009).
[24]A. C. Ferrari, J. C. Meyer, V. Scardaci, C. Casiraghi, M. Lazzeri, F. Mauri, S. Piscanec, D. Jiang, K. S. Novoselov, S. Roth, and A. K. Geim, Phys. Rev. Lett. **97**, 187401 (2006).
[25]L. M. Malard, M. A. Pimenta, G. Dresselhaus, and M. S. Dresselhaus, Phys. Rep. **473**, 51 (2009).
[26]I. Calizo, I. Bejenari, M. Rahman, L. Guanxiong, and A. A. Balandin, J. Appl. Phys. **106**, 043509 (2009).
[27]Y. F. Hao, Y. Wang, L. Wang, Z. Ni, Z. Wang, R. Wang, C. K. Koo, Z. Shen, and J. T. L. Thong, Small **6**, 195 (2010).
[28]Z. H. Ni, Y. Y. Wang, T. Yu, and Z. X. Shen, Nano Res. **1**, 273 (2008).
[29]Z. H. Ni, L. A. Poromarenko, R. R. Nair, R. Yang, S. Anissimova, I. V. Grigorieva, F. Schedin, P. Blake, Z. X. Shen, E. H. Hill, K. S. Novoselov, and A. K. Geim, Nano Lett. **10**, 3868 (2010).
[30]C. H. Lui, Z. Li, Z. Chen, P. V. Klimov, L. E. Brus, and T. F. Heinz, Nano Lett. **11**, 164 (2011).
[31]Y. Zhang, Z. Jiang, J. P. Small, M. S. Purewal, Y. W. Tan, M. Fazlollahi, J. D. Chudow, J. A. Jaszczak, H. L. Stormer, and P. Kim, Phys. Rev. Lett. **96**, 136806 (2006).
[32]D. V. Khveshchenko, Phys. Rev. Lett. **87**, 206401 (2001).
[33]M. Koshino and E. McCann, Phys. Rev. B. **83**, 165443 (2011).
[34]X. Z. Yan and C. S. Ting, Phys. Rev. Lett. **101**, 126801 (2008).
[35]E. McCann, K. Kechedzhi, V. I. Fal'ko, H. Suzuura, T. Ando, and B. L. Altshuler, Phys. Rev. Lett. **97**, 146805 (2006).
[36]V. I. Fal'ko, K. Kechedzhi, E. McCann, B. L. Altshuler, H. Suzuura, and T. Ando, Solid State Commun. **143**, 33 (2007).
[37]J. Moser, H. Tao, S. Roche, F. Alzina, C. M. S. Torres, and A. Bachtold, Phys. Rev. B **81**, 205445 (2010).
[38]J. Eroms and D. Weiss, New J. Phys. **11**, 095021 (2009).
[39]W. Zhu, V. Perebeinos, M. Freitag, and P. Avouris, Phys. Rev. B **80**, 235402 (2009).